Heterobimetallic Dinitrogen Complexes That Contain the $\{[N_3N]Mo-N{=}N\}^-$ Ligand

Myra B. O'Donoghue,[†] William M. Davis,[†] Richard R. Schrock,*[,†] and William M. Reiff*[,‡]

Department of Chemistry 6-331, Massachusetts Institute of Technology, Cambridge, Massachusetts 02139, and Department of Chemistry, Northeastern University, 360 Huntington Avenue, Boston, Massachusetts 02115

Received September 17, 1998

$\{[N_3N]Mo-N{=}N\}_2Mg(THF)_2$ reacts with $FeCl_2$ at −20 °C in a mixture of ether, THF, and toluene to yield paramagnetic $\{[N_3N]Mo-N{=}N\}_3Fe$ (**1**), an X-ray study of which shows it to contain iron in a trigonal planar environment. X-band ESR, iron-57 Mössbauer spectroscopy, and magnetic susceptibility studies of **1** confirm that it contains high-spin Fe(III) in an anisotropic magnetic environment. Addition of DMPE to toluene solutions of **1** results in loss of $[N_3N]MoN_2$ from the coordination sphere to give $\{[N_3N]Mo-N{=}N\}_2Fe(DMPE)$ (**2**). SQUID magnetic susceptibility and Mössbauer data are in accord with formulation of **2** as a high-spin Fe(II) complex. $\{[N_3N]Mo-N{=}N\}_2Mg(THF)_2$ reacts with $VCl_4(DME)$ and $VCl_3(THF)_3$ in THF to give paramagnetic $\{[N_3N]Mo-N{=}N\}_3VCl$ (**3**) in 28−42% yield. A second paramagnetic complex is also produced in these reactions and has been identified by X-ray crystallography as $\{[N_3N]Mo-N{=}N\}_2VCl(THF)$ (**4**). Several zirconium/molybdenum dinitrogen complexes have been prepared by the reaction between $\{[N_3N]Mo-N{=}N\}_2Mg(THF)_2$ and $ZrCl_4(THF)_2$, and $\{[N_3N]Mo-N{=}N\}_2ZrCl_2$ has been characterized by X-ray crystallography.

Introduction

We recently reported that $\{[N_3N]Mo(N_2)\}_2Mg(THF)_2$ could be prepared by reducing $[N_3N]MoCl$ with magnesium in THF[1] and in a preliminary manner that $\{[N_3N]Mo(N_2)\}_2Mg(THF)_2$ reacts with $FeCl_2$ to give trigonal planar $\{[N_3N]Mo(N_2)\}_3Fe$.[2] $\{[N_3N]Mo(N_2)\}^-$ can be viewed as a Mo(IV) complex of the diazenido(2−) ligand, i.e., $[N_3N]Mo-N{=}N^-$, in which 8 electrons are found in the degenerate π orbitals formed from the d_{xz} and d_{yz} orbitals on Mo (where Mo−N−N is the *z* axis) and two orthogonal p orbitals on each nitrogen atom. Therefore $\{[N_3N]Mo(N_2)\}^-$ is related to N_3^-, which also has 8 electrons in its π MO system. We became interested in preparing other examples of transition metal complexes that contain the $\{[N_3N]Mo(N_2)\}^-$ ligand and in exploring a complicating feature of the use of $\{[N_3N]Mo(N_2)\}^-$ as a ligand, namely the fact that its one-electron oxidation product, $[N_3N]Mo(N_2)$, is also a stable species.[1] The results of these experiments are reported here.

Results and Discussion

Synthesis of Iron/Molybdenum Dinitrogen Complexes. Addition of $FeCl_2$ to $\{[N_3N]Mo(N_2)\}_2Mg(THF)_2$ dissolved in a 10:2:1 mixture of ether, THF, and toluene, led to a darkening of the solution over the course of 15 min. $\{[N_3N]Mo(N_2)\}_3Fe$ (**1**) can be isolated in 38% yield from the pentane extract of the crude reaction product as plum-colored, paramagnetic crystals. A black magnetic solid is formed during the course of the reaction (it clings to the stir bar) that we assume to be iron. Therefore the ideal stoichiometry for the reaction to give **1** would be that shown in eq 1. The ^1H NMR spectrum of **1** in

$$\{[N_3N]Mo-N{=}N\}_2Mg(THF)_2 + FeCl_2 \xrightarrow[-\,MgCl_2\,-\,{}^1/_3Fe^\circ]{\text{ether/THF/toluene}} {}^2/_3\{[N_3N]Mo-N{=}N\}_3Fe \quad (1)$$

C_6D_6 exhibits three broad, shifted resonances at 9.25, −9.71, and −64.0 ppm, consistent with a species in which the $[N_3N]Mo$ portion of the molecule is C_3-symmetric.[1,3] An IR spectrum of **1** in Nujol shows primarily an absorption at 1703 cm^{-1}, with weaker absorptions between 1703 and 1600 cm^{-1}, suggesting that dinitrogen is present and acting as a diazenido(2−) ligand. The UV−visible spectrum of **1** in pentane has an intense absorption at 516 nm (ϵ = 22 800 M^{-1} cm^{-1}) that shifts to 476 nm upon addition of THF (see below). Satisfactory elemental analyses of **1** have not been obtained due to the presence of trace amounts of $[N_3N]Mo(N_2)$ in the samples.

The molecular structure of **1** was elucidated in an X-ray crystallographic study. Crystals of **1** were grown from saturated pentane solutions at −20 °C; a quarter of a molecule of pentane was found in the unit cell. Crystallographic data are given in Table 1. A view of the molecular structure of **1** along with the atom-labeling scheme is shown in Figure 1, while pertinent bond lengths and bond angles are listed in Table 2. The molecule is a rare example of a complex with iron in a trigonal planar environment. The $[N_3N]Mo(N_2)$ unit can be viewed as a bulky ligand in which the TMS groups preclude higher coordination numbers. The three Mo−N−N linkages are essentially linear, as are two of the Fe−N−N linkages. However, one of the Mo−N−N−Fe linkages is significantly bent at the nitrogen bound to iron (Fe−N(2)−N(1) = 156(2)°). The deviation from linearity

[†] MIT.
[‡] Northeastern University.

(1) O'Donoghue, M. B.; Schrock, R. R.; Davis, W. M. *Inorg. Chem.* **1998**, *37*, 5149.
(2) O'Donoghue, M. B.; Zanetti, N. C.; Davis, W. M.; Schrock, R. R. *J. Am. Chem. Soc.* **1997**, *119*, 2753.
(3) Schrock, R. R.; Seidel, S. W.; Mösch-Zanetti, N. C.; Shih, K.-Y.; O'Donoghue, M. B.; Davis, W. M.; Reiff, W. M. *J. Am. Chem. Soc.* **1997**, *119*, 11876.

10.1021/ic9811188 CCC: $18.00
Published on Web 12/30/1998

Table 1. Crystallographic Data, Collection Parameters, and Refinement Parameters for $\{[N_3N]Mo{-}N{=}N\}_3Fe$ (**1**), $\{[N_3N]Mo{-}N{=}N\}_2VCl(THF)$ (**4**), and $\{[N_3N]Mo{-}N{=}N\}_2ZrCl_2$ (**6**)[a]

	1	**4**	**6**
empirical formula	$C_{46.25}H_{120}FeMo_3N_{18}Si_9$	$C_{39}H_{98.50}ClMo_2N_{12}O_{2.25}Si_6V$	$C_{32}H_{88}Cl_2Mo_2N_{12}O_{0.50}Si_6Zr$
fw	1529.44	1218.61	1171.68
space group	$P\bar{1}$	$P2_1/n$	$P2_1/c$
a (Å)	10.4926(2)	14.16110(10)	16.4150(3)
b (Å)	14.3300(10)	21.61220(10)	18.5686(4)
c (Å)	26.8875(6)	21.1463(3)	19.8964(4)
α (deg)	97.2850(10)	90	90
β (deg)	93.2670(10)	98.6770(10)	100.2590(10)
γ (deg)	90.163(2)	90	90
V (Å^3), Z	4001.93(12), 2	6397.81(11), 4	5967.5(2), 4
D_{calc} (g/cm^3)	1.262	1.265	1.304
μ (cm^{-1})	8.11	7.23	8.29
R1, wR2 [$I > 2\sigma(I)$][b]	0.1345, 0.2611	0.0660, 0.1410	0.0559, 0.1322
R1, wR2 (all data)[c]	0.1896, 0.3082	0.1080, 0.1705	0.0986, 0.1835

[a] All data were collected on a Siemens SMART/CCD meter at 183 K using 0.710 73 Å Mo Kα radiation and solved as described in ref 35. [b] $R1 = \sum||F_o| - |F_c||/\sum|F_o|$. [c] $wR2 = [(\sum[w(F_o^2 - F_c^2)^2]/\sum[w(F_o^2)^2]]^{1/2}$.

Table 2. Selected Bond Lengths and Bond Angles for $\{[N_3N]Mo(N_2)\}_3Fe$ (**1**)

Bond Lengths (Å)					
Fe−N(2)	1.86(2)	Fe−N(4)	1.84(2)	Fe−N(6)	1.82(2)
Mo(1)−N(1)	1.86(2)	Mo(2)−N(3)	1.81(2)	Mo(3)−N(5)	1.82(2)
N(1)−N(2)	1.20(3)	N(3)−N(4)	1.25(2)	N(5)−N(6)	1.27(2)
Mo(1)−N(11)	1.97(2)	Mo(2)−N(23)	2.03(2)	Mo(3)−N(32)	2.00(2)
Mo(1)−N(14)	2.24(2)	Mo(2)−N(24)	2.26(2)	Mo(3)−N(34)	2.24(2)
Bond Angles (deg)					
Mo(1)−N(1)−N(2)	174(2)	Mo(2)−N(3)−N(4)	175(2)		
Mo(3)−N(5)−N(6)	179(2)	Fe−N(2)−N(1)	156(2)		
Fe−N(4)−N(3)	175(2)	Fe−N(6)−N(5)	176(2)		
Mo(1)−N(11)−Si(11)	127.4(12)	Mo(2)−N(23)−Si(23)	123.7(10)		
N(2)−Fe−N(4)	114.0(9)	N(2)−Fe−N(6)	119.2(10)		
N(4)−Fe−N(6)	126.8(9)				
Dihedral Angles (deg)[a]					
N(14)−Mo(1)−N(11)−Si(11)	170.4	N(14)−Mo(1)−N(13)−Si(13)	142.5		
N(14)−Mo(1)−N(12)−Si(12)	−164.7	N(24)−Mo(2)−N(23)−Si(23)	176.3		
N(34)−Mo(3)−N(32)−Si(32)	−177.9				

[a] Obtained from a Chem-3D model.

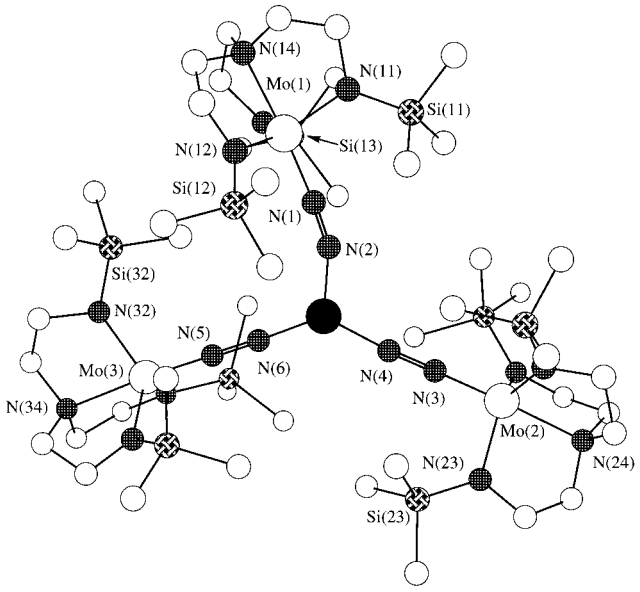

Figure 1. View of the structure of $\{[N_3N]Mo{-}N{=}N\}_3Fe$ (**1**) with the trigonal plane lying in the plane of the paper.

of Fe−N(2)−N(1) may be solely a consequence of steric crowding created by the $[N_3N]^{3-}$ ligand. In previous work,[3] it has been found that the twisting of a given TMS group out of the $N_{ax}-M-N_{eq}$ plane and the resulting decrease in the $N_{ax}-M-N_{eq}-Si$ dihedral angle are useful measures of the degree of steric strain in the pocket of $[N_3N]$ complexes. In **1** the dihedral angle defined by N(14)−Mo(1)−N(13)−Si(13) is found to be 142.5°, indicative of some steric pressure arising from three $[N_3N]Mo(N_2)$ units lying in the trigonal plane. However, all other $N_{ax}-M-N_{eq}-Si$ dihedral angles are close to 180°. In view of the relatively large errors we cannot say that distances within the $[N_3N]Mo(N_2)$ units are significantly different. Nevertheless, the N−N bond distances suggest that the dinitrogen in the ligands in **1** is substantially reduced compared to free dinitrogen (1.098 Å), approximately to the diazenido (N_2^{2-} or Mo−N=N−Fe) stage.

Known three-coordinate iron complexes can be grouped into three broad classes, namely, dimeric Fe(II) complexes such as $[Fe(O\text{-}2,4,6\text{-}t\text{-}Bu_3C_6H_2)_2]_2$[4] and $[Fe(NPh_2)_2]_2$,[5] which contain terminal and bridging alkoxy or amide ligands, monomeric Fe(II) complexes such as $Fe[N(SiMe_3)_2]_2(THF)$[5] and $\{Fe[N(SiMe_3)_2]_3\}^-$,[6−10] and monomeric Fe(III) complexes, of which only two other examples, $Fe(NRAr)_3$ (R = $C(CD_3)_2CH_3$, Ar =

(4) Bartlett, R. A.; Ellison, J. J.; Power, P. P.; Shoner, S. C. *Inorg. Chem.* **1991**, *30*, 2888.
(5) Olmstead, M. M.; Power, P. P.; Shoner, S. C. *Inorg. Chem.* **1991**, *30*, 0, 2547.
(6) Bradley, D. C.; Hursthouse, M. B.; Rodesiler, P. F. *Chem. Commun.* **1969**, 14.
(7) Alyea, E. C.; Bradley, D. C.; Copperthwaite, R. G.; Sales, K. D. *J. Chem. Soc., Dalton Trans.* **1973**, 185.
(8) Bradley, D. C. *Inorg. Synth.* **1978**, *18*, 112.
(9) Bradley, D. C.; Copperthwaite, R. G.; Cotton, S. A.; Sales, K. D. *J. Chem. Soc., Dalton Trans.* **1973**, 191−194.

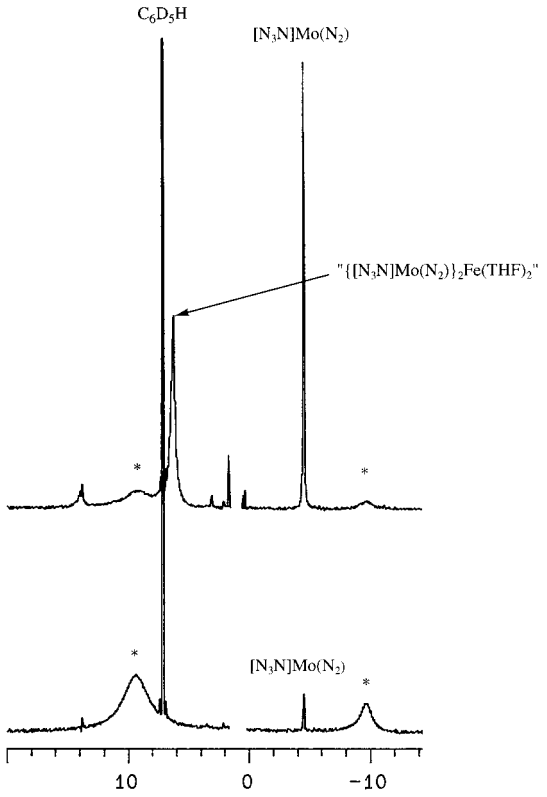

Figure 2. ^{1}H NMR spectrum of $\{[N_3N]Mo{-}N{=}N\}_3Fe$ in C_6D_6 (lower spectrum) and after addition of 10 equiv of THF-d_8 (upper spectrum; * = $\{[N_3N]Mo(N_2)\}_3Fe$).

3,5-$C_6H_3Me_2$)[11] and $Fe[N(SiMe_3)_2]_3$,[6−10] are known. Complex **1** is unique among these trigonal complexes for several reasons. First, crystallographically characterized, heterobimetallic complexes containing bridging dinitrogen are rare[12−14] and to our knowledge **1** is the only reported example of a structurally characterized iron−molybdenum dinitrogen complex, a type of species that is perhaps relevant to the reduction of dinitrogen in view of the structure of Fe/Mo nitrogenase in one resting state.[15] Second, the three ligands coordinated to iron are all derived from dinitrogen. Finally, the dinitrogen-containing ligands can exist in either an anionic form, $\{[N_3N]Mo(N_2)\}^-$, or a neutral form, $[N_3N]Mo(N_2)$.[2] Therefore there is some question concerning the oxidation state of a metal to which such a ligand is bound.

The reaction that produces **1** turns out to be relatively complex and its outcome is sensitive to temperature and solvent. For example, if the reaction is carried out at room temperature in THF the main product is $[N_3N]Mo(N_2)$, suggesting that oxidation of $\{[N_3N]Mo(N_2)\}_2Mg(THF)_2$ occurs exclusively (eq 2). If the reaction is conducted at low temperature in THF, the major species produced is "$[N_3N]Mo{-}N{=}N\}_2Fe(THF)_2$" according to ^{1}H NMR spectroscopy.

$$\{[N_3N]Mo{-}N{=}N\}_2Mg(THF)_2 + FeCl_2 \xrightarrow[-\,MgCl_2]{THF} 2[N_3N]Mo(N_2) + Fe^\circ \quad (2)$$

Toluene and pentane solutions of **1** are an intense purple color, whereas THF solutions are orange-brown. The intense absorption at 516 nm (ϵ = 22 800 M^{-1} cm^{-1}) in the UV−visible spectrum of **1** in pentane shifts to 476 nm upon addition of THF. Although NMR spectra contain only broad resonances, NMR spectra are useful in monitoring species in solution. The lower half of Figure 2 shows a portion of the ^{1}H NMR spectrum of **1** in C_6D_6. The broad resonance at 9.25 ppm is assigned to the TMS groups of the TREN ligand and the resonance at −9.71 ppm is attributed to one set of the methylene protons of the ligand backbone. The relatively sharp resonance at −4.5 ppm is due to the TMS groups in a small amount of $[N_3N]Mo(N_2)$ present in the sample. Upon addition of 10 equiv of THF-d_8 to the sample, the color changed from purple to orange-brown and the upper spectrum in Figure 2 is obtained. The resonance at 9.25 ppm has decreased significantly in intensity, the resonance assigned to $[N_3N]Mo(N_2)$ has increased dramatically in intensity, and a new resonance at 6.57 ppm has grown in. The increase in the intensity of the resonance at −4.5 ppm suggests that THF displaces $[N_3N]Mo(N_2)$ from the iron center and that Fe(III) is thereby reduced to Fe(II). Most likely the Fe(II) complex, if it is a monomer, would be a tetrahedral species, namely $\{[N_3N]Mo(N_2)\}_2Fe(THF)_2$ (eq 3). Reduction of **1** by THF is reversible; by ^{1}H NMR spectroscopy it is clear that $\{[N_3N]Mo(N_2)\}_2Fe(THF)_2$ reacts with $[N_3N]Mo(N_2)$ to give free THF and **1**. Similar redox behavior has been found in vanadium/molybdenum dinitrogen complexes (see below).

$$\{[N_3N]Mo{-}N{=}N\}_3Fe \underset{-\,THF}{\overset{+\,THF}{\rightleftharpoons}} \{[N_3N]Mo{-}N{=}N\}_2Fe(THF)_2 + [N_3N]Mo(N_2) \quad (3)$$

There are two plausible mechanisms for the formation of **1**. Nucleophilic substitution and redox reactions might occur at comparable rates to generate $\{[N_3N]Mo(N_2)\}_2Fe(THF)_2$ (eq 4) and $[N_3N]Mo(N_2)$ (eq 2) in solution. $\{[N_3N]Mo(N_2)\}_2Fe(THF)_2$

$$\{[N_3N]Mo{-}N{=}N\}_2Mg(THF)_2 + FeCl_2 \xrightarrow{-\,MgCl_2} \{[N_3N]Mo{-}N{=}N\}_2Fe(THF)_2 \quad (4)$$

$$1.5\{[N_3N]Mo{-}N{=}N\}_2Mg(THF)_2 + FeCl_2 \xrightarrow{-\,0.5MgCl_2} \text{“}\{[N_3N]Mo{-}N{=}N\}_3Fe\}\{MgCl\}\text{”} \quad (5)$$

then reacts with $[N_3N]Mo(N_2)$ to yield **1**. The observed reaction of $\{[N_3N]Mo(N_2)\}_2Mg(THF)_2$ with $FeCl_2$ at room temperature to yield $[N_3N]Mo(N_2)$ and the reaction of $\{[N_3N]Mo(N_2)\}_2Fe(THF)_2$ with $[N_3N]Mo(N_2)$ to give free THF and **1** suggest that such a scenario is plausible. Alternatively, if the rate of nucleophilic substitution is faster than the rate at which $\{[N_3N]Mo(N_2)\}_2Mg(THF)_2$ is oxidized, then "$\{([N_3N]Mo(N_2))_3Fe\}^-\{MgCl\}^+$" might be generated (eq 5) and subsequently oxidized by $FeCl_2$ to give **1**. Interestingly, $Fe(NRAr)_3$ (R = $C(CD_3)_2CH_3$, Ar = 3,5-$C_6H_3Me_2$) is synthesized by oxidation of the "ate" complex $(ArRN)Fe(\mu\text{-}NRAr)_2Li(OEt_2)$.[11] Attempts to prepare **1** by addition of $FeCl_3$ to THF solutions of $\{[N_3N]Mo(N_2)\}_2Mg(THF)_2$ led only to complex product mixtures. Among the products identifiable by ^{1}H NMR spectroscopy were $[N_3N]MoCl$, $[N_3N]Mo(N_2)$ and $\{[N_3N]Mo(N_2)\}_2Fe(THF)_2$, along with **1** and unreacted $\{[N_3N]Mo(N_2)\}_2Mg(THF)_2$. On the basis of the data in hand it is not possible at this stage to determine which of the proposed methods of forming **1** is the fastest.

(10) Eller, P. G.; Bradley, D. C.; Hursthouse, M. B.; Meek, D. W. *Coord. Chem. Rev.* **1977**, *24*, 1.
(11) Stokes, S. L.; Davis, W. M.; Odom, A. L.; Cummins, C. C. *Organometallics* **1996**, *15*, 4521.
(12) Hidai, M.; Mizobe, Y. *Chem. Rev.* **1995**, *95*, 1115.
(13) Richards, R. L. *Chem. Br.* **1988**, *24*, 133.
(14) Henderson, R. A.; Leigh, G. J.; Pickett, C. J. *Adv. Inorg. Chem. Radiochem.* **1983**, *27*, 197.
(15) Chan, M. K.; Kim, J. S.; Rees, D. C. *Science* **1993**, *260*, 792.

Efforts to isolate $\{[N_3N]Mo(N_2)\}_2Fe(THF)_2$ have not been successful. However, addition of DMPE (1,2-bisdimethylphosphinoethane) to a toluene solution of **1** gave $\{[N_3N]Mo-N{=}N\}_2Fe(DMPE)$ (**2**), which could be isolated as black blocks from diethyl ether in moderate (43%) yield based on the number of equivalents of $\{[N_3N]Mo(N_2)\}_2Mg(THF)_2$ used to generate **1** (eq 6). We presume that $\{[N_3N]Mo(N_2)\}_2Fe(THF)_2$ cannot

$$\{[N_3N]Mo-N{=}N\}_3Fe \xrightarrow[\text{toluene}]{\text{DMPE}} \{[N_3N]Mo-N{=}N\}_2Fe(DMPE) + [N_3N]Mo(N_2) \quad (6)$$

be isolated from THF as a consequence of its high solubility and the ready exchange of the THF ligands. Attempts to isolate $\{[N_3N]Mo(N_2)\}_2Fe(THF)_2$ from solvents such as pentane led to its disproportionation to **1** and iron metal. An attempted X-ray study of **2** showed it to be a tetrahedral complex, but a disorder in the trimethylsilyl groups of the $[N_3N]^{3-}$ ligand prevented satisfactory refinement.

The ^{1}H NMR spectrum of **2** in C_6D_6 consists of five broad resonances between +40 and −118 ppm for the five types of protons present. The resonance at 6.62 ppm is assigned to the TMS groups, the resonances at −4.67 and −47.43 ppm are assigned to the ligand methylene resonances, and the resonances at +37.00 and −117.46 ppm are assigned to the methyl and methylene protons of the DMPE ligand. No resonance could be located in the ^{31}P NMR spectrum of **2** as a consequence of the proximity of the phosphorus nuclei to the paramagnetic iron center. The IR spectrum of **2** has a strong, sharp band at 1706 cm^{-1} that is assigned to ν_{NN}, while the UV−visible spectrum has two intense absorptions at 360 nm (ϵ = 23 306 M^{-1} cm^{-1}) and 508 nm (ϵ = 13 997 M^{-1} cm^{-1}) that are unaffected upon addition of THF, consistent with no displacement of THF from the coordination sphere to give $\{[N_3N]Mo(N_2)\}_2Fe(THF)_2$, and in contrast to the behavior of **1**. However, **2** apparently decomposes rapidly in the solid state when exposed to high vacuum as evidenced by a color change from purple to dark brown. We speculate that loss of DMPE is the first step in this decomposition although no products of the reaction have been identified. The reaction between $Fe(DMPE)Cl_2$ and $\{[N_3N]Mo(N_2)\}_2Mg(THF)_2$ in THF over the course of 12 h turned deep green and then purple as a mixture of **2** and $[N_3N]Mo(N_2)$ was formed (according to NMR spectra). However, **2** could not be isolated in good yield from this reaction mixture.

Synthesis of Vanadium/Molybdenum Dinitrogen Complexes. $VCl_4(DME)$ reacts with 1.5 equiv of $\{[N_3N]Mo(N_2)\}_2Mg(THF)_2$ in THF to yield deep purple solutions. ^{1}H NMR spectra of the crude reaction mixture reveal the presence of two paramagnetic and one diamagnetic species, as well as traces of $[N_3N]Mo(N_2)$,[2] $[N_3N]MoH$,[3] and $[bitN_3N]Mo$,[3] a complex in which a methylene group bridges between Mo and Si. Paramagnetic $\{[N_3N]Mo(N_2)\}_3VCl$ (**3**) can be separated from the reaction mixture by crystallization from THF/pentane as black plates and has been isolated in 42% yield. The actual yield of **3** is higher according to ^{1}H NMR spectra of the mother liquor. The connectivity of **3** has been established by a single-crystal diffraction study of low resolution (1.6 Å), which shows three $[N_3N]Mo(N_2)$ ligands and one chloride ligand bound to a pseudo-tetrahedral vanadium center.[16] The ^{1}H NMR spectrum of **3** consists of three relatively sharp resonances at 1.36 ($\Delta\nu_{1/2}$ = 14 Hz), 0.94 ($\Delta\nu_{1/2}$ = 6 Hz) and −0.55 ppm ($\Delta\nu_{1/2}$ = 14 Hz) with the resonance at 0.94 ppm being assigned to the TMS groups of the ligand. Solutions of **3** in C_6D_6 remain unchanged when stored under dinitrogen for 3 days (according to ^{1}H NMR spectroscopy). The IR spectrum of **3** in Nujol exhibits a broad N−N stretch at 1579 cm^{-1}, and the UV−visible spectrum of **3** in pentane has an intense absorption at 540 nm (ϵ = 29 787 M^{-1} cm^{-1}). SQUID[17] magnetic susceptibility measurements on solid **3** show that it behaves as a Curie paramagnet between 300 and 5 K with μ = 1.50(1) μ_B (R = 0.9998), in accord with its formulation as a d^1 V(IV) complex. The second paramagnetic species that is present in the reaction mixture is characterized by broad resonances at 6.00, 1.28, and −5.56 ppm. On the basis of the results of reactions between $VCl_3(THF)_3$ and $\{[N_3N]Mo(N_2)\}_2Mg(THF)_2$ (see below) this complex is formulated as the V(III) complex $\{[N_3N]Mo(N_2)\}_2VCl(THF)$ (**4**). It cannot be isolated from reaction mixtures prepared in this manner.

The reaction between $VCl_3(THF)_3$ and 1 equiv of $\{[N_3N]Mo(N_2)\}_2Mg(THF)_2$ in THF also yields deep purple solutions from which **3** can be isolated in 28% yield. The formation of **3** suggests that some species is reduced during the course of the reaction. We have not been able to confirm that vanadium is also the reducing agent, as no reduced vanadium species (less than V(III)) could be isolated from the reaction mixture or identified in mixtures. The complex proton NMR spectra of the crude reaction mixture suggest that **3** and **4**, along with traces of $[N_3N]MoH$, $[bitN_3N]$, and $[N_3N]Mo(N_2)$ are present.

The reaction between $VCl_3(THF)_3$ and 1.5 equiv of $\{[N_3N]Mo(N_2)\}_2Mg(THF)_2$ produces red-purple solutions (as opposed to the deep purple solutions observed in reactions involving 1 equiv of $\{[N_3N]Mo(N_2)\}_2Mg(THF)_2$) and ^{1}H NMR spectra again reveal the presence of **3** and **4**, as well as trace amounts of $[N_3N]MoH$, $[bitN_3N]$, and $[N_3N]Mo(N_2)$. Resonances at −0.55 ppm (for **3**) and −5.56 ppm (for **4**) integrate in a ratio of 1:2, suggesting that **4** is formed in higher yield than in the reaction between $VCl_4(DME)$ and 1.5 equiv of $\{[N_3N]Mo(N_2)\}_2Mg(THF)_2$, where the resonances integrate in the ratio of approximately 2:1. After several hours, C_6D_6 solutions of the mixture of **3** and **4** take on a deep purple color. Proton NMR spectra of these purple solutions reveal that resonances attributable to **4**, most noticeably those at 1.28 and −5.56 ppm, have diminished in intensity, while the resonances for **3** have increased. These results suggest that **4** is unstable under the reaction conditions, undergoing formally a disproportionation reaction to yield **3** as one of the products (eq 7). No other (potentially reduced) vanadium products of this reaction could be identified.

$$\{[N_3N]Mo-N{=}N\}_2VCl(THF) \rightarrow \{[N_3N]Mo-N{=}N\}_3VCl + ? \quad (7)$$

By analogy with the reaction between $\{[N_3N]Mo(N_2)\}_2Fe(THF)_2$ and $[N_3N]Mo(N_2)$ to yield **1**, **4** should react with $[N_3N]Mo(N_2)$ to yield **3**. The ^{1}H NMR spectrum of a mixture of **3** and **4** is shown in Figure 3 (lower spectrum), while the same sample to which $[N_3N]Mo(N_2)$ has been added is shown in the upper spectrum. Upon addition of $[N_3N]Mo(N_2)$ to the mixture of **3** and **4** an immediate color change to deep purple is observed and resonances attributable to **4** are no longer visible, while resonances for **3** have increased significantly in intensity. These results are consistent with coordination of $[N_3N]Mo(N_2)$ to **4** to give **3** (eq 8). Upon addition of THF-d_8 (∼400 equiv)

$$\underset{\mathbf{4}}{\{[N_3N]Mo(N_2)\}_2VCl(THF)} + [N_3N]Mo(N_2) \xrightarrow[-\text{ THF}]{C_6D_6} \underset{\mathbf{3}}{\{[N_3N]Mo(N_2)\}_3VCl} \quad (8)$$

to C_6D_6 solutions of **3**, resonances attributable to trace amounts

(16) Crystallographic information is available upon request.
(17) O'Connor, C. J. *Prog. Inorg. Chem.* **1982**, *29*, 203.

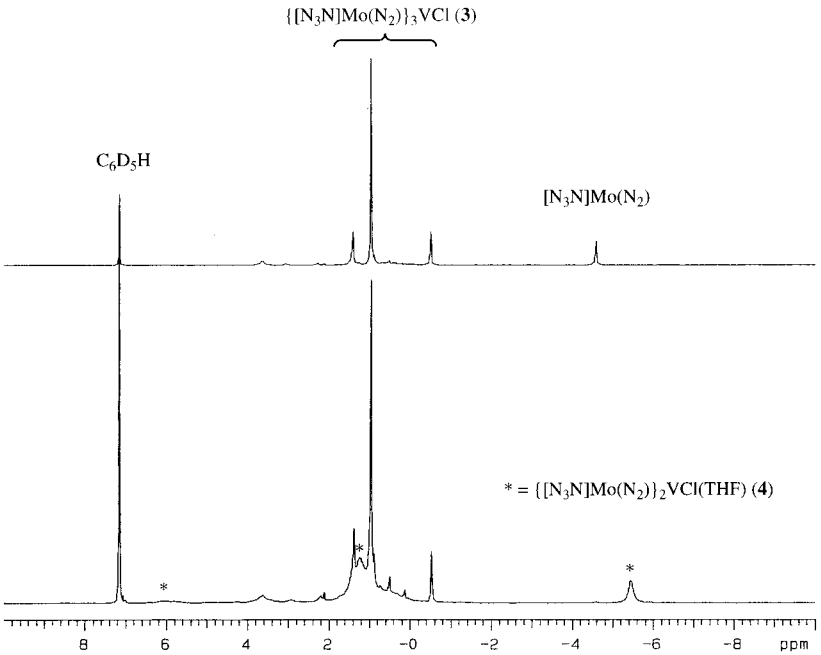

Figure 3. ^{1}H NMR spectrum of a mixture of **3** and **4** in C_6D_6 (lower spectrum) and after addition of $[N_3N]Mo(N_2)$ (upper spectrum).

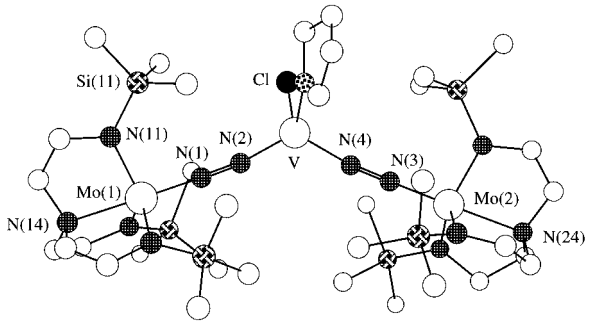

Figure 4. View of the structure of $\{[N_3N]Mo{-}N{=}N\}_2VCl(THF)$ (**4**).

of $[N_3N]Mo(N_2)$ and **4** are observed in the ^{1}H NMR spectrum. However, after 24 h the main species present in solution is **3**. These results suggest that $[N_3N]Mo(N_2)$ can be displaced from **3** to give **4**, but the equilibrium lies toward **3**. The fact that a mixture of **3** and **4** in THF take on the deep purple color characteristic of **3** relatively slowly might be ascribed to a slower reaction between **4** and $[N_3N]Mo(N_2)$ in THF than in C_6D_6.

Attempts to prepare vanadium complexes analogous to $\{[N_3N]Mo(N_2)\}_3Fe$ from $VCl_3(THF)_3$ and $\{[N_3N]Mo(N_2)\}_2Mg(THF)_2$ led only to mixtures that contain **3** and **4**, along with $[N_3N]Mo(N_2)$ and traces of $[N_3N]MoH$ and $[bitN_3N]Mo$. Therefore we believe that $\{[N_3N]Mo(N_2)\}_3V$ is not accessible by this route, perhaps as a consequence of the presence of chloride. An attempt to synthesize $\{[N_3N]Mo(N_2)\}_4V$ from $VCl_4(DME)$ and 2 equiv of $\{[N_3N]Mo(N_2)\}_2Mg(THF)_2$ in THF at −20 °C yielded similar complex mixtures. However, $\{[N_3N]Mo(N_2)\}_4V$ is likely to be inaccessible also for steric reasons, as suggested by studies involving the synthesis of Zr complexes described below.

Although the instability of **4** in solution has precluded its isolation on a preparative scale, crystals of **4** suitable for an X-ray diffraction study were obtained from a mixture of THF and diethyl ether at −20 °C. Crystallographic data and collection and refinement parameters are given in Table 1. The molecular structure of **4** along with the atom-labeling scheme is shown in Figure 4. Selected bond lengths and bond angles are listed in Table 3 along with analogous distances and angles in $\{[N_3N]Mo(N_2)\}_2Mg(THF)_2$[1,2] for comparison. Diethyl ether (1.25 per V) was found in the unit cell. **4** is composed of two $\{[N_3N]Mo(N_2)\}^-$ units bound to pseudo-tetrahedral vanadium, the coordination sphere being completed by one THF and one chloride. The N−V−N bond angle is only 119.8°, compared to 134.7° for the N−Mg−N angle in $\{[N_3N]Mo(N_2)\}_2Mg(THF)_2$, even though V(3+) is smaller (0.64 Å) than Mg(2+) (0.72 Å)[18] and the V−N bonds in **4** are shorter than the Mg−N bonds. The Mo−N−N linkages are essentially linear and the N−N bond lengths (1.217(7) and 1.221(7) Å) are consistent with a greater degree of reduction of the N_2 fragment in **4** than in $\{[N_3N]Mo(N_2)\}_2Mg(THF)_2$; the N−N distances are consistent with formulation of **4** as a diazenido complex[12−14] with Mo and V in formal oxidation states of 4+ and 3+, respectively. The N_{ax}−Mo−N_{eq}−Si dihedral angles are all close to 180° (not listed) in all compounds in Table 3, consistent with little steric congestion in the trigonal pocket defined by the $[N_3N]^{3-}$ ligand. These distances and angles should be compared with those in related homobimetallic vanadium complexes[19−22] such as $[(Me_3CCH_2)_3V]_2(\mu\text{-}N_2)$,[22] $[CH_3C\{(CH_2)N(i\text{-}Pr)\}_3V]_2(\mu\text{-}N_2)$,[20] or $[(i\text{-}Pr_2N)_3V]_2(\mu\text{-}N_2)$.[21] The N−N bonds in **4** are slightly shorter than the corresponding bonds in the homobimetallic complexes (∼1.26 Å), while the V−N bond lengths of the homobimetallic complexes (∼1.72 Å) are significantly shorter than those in **4**.

Synthesis of Zirconium/Molybdenum Dinitrogen Complexes. Our excursions into iron and vanadium chemistry coupled with the observation that reactions of $\{[N_3N]Mo(N_2)\}_2Mg(THF)_2$ with halides of transition metals such as palladium, nickel, and zinc proceed via oxidative pathways yielding $[N_3N]Mo(N_2)$[1] have made it clear that $\{[N_3N]Mo(N_2)\}^-$ is relatively easily oxidized by a readily reduced first-row or late transition metal. Therefore it seemed reasonable to attempt to

(18) Shannon, R. D. *Acta Crystallogr.* **1974**, *A32*, 751.
(19) Edema, J. J. H.; Meetsma, A.; Gambarotta, S. *J. Am. Chem. Soc.* **1989**, *111*, 6878.
(20) Desmangles, N.; Jenkins, H.; Ruppa, K. B.; Gambarotta, S. *Inorg. Chim. Acta* **1996**, *250*, 1.
(21) Song, J.-I.; Berno, P.; Gambarotta, S. *J. Am. Chem. Soc.* **1994**, *116*, 6927.
(22) Buijink, J.-K. F.; Meetsma, A.; Teuben, J. H. *Organometallics* **1993**, *12*, 2004.

Table 3. Selected Bond Lengths and Bond Angles for $\{[N_3N]Mo{-}N{=}N\}_2Mg(THF)_2$,[a] $\{[N_3N]Mo{-}N{=}N\}_2VCl(THF)$ (**4**), and $\{[N_3N]Mo{-}N{=}N\}_2ZrCl_2$ (**6**)

	$\{[N_3N]Mo{-}N{=}N\}_2Mg(THF)_2$	**4**	**6**
Mo(1)−N(1)	1.876(11)	1.836(6)	1.797(6)
Mo(1)−N(11)	1.998(12)	2.012(6)	1.988(6)
Mo(1)−N(12)	2.001(11)	2.004(6)	1.975(7)
Mo(1)−N(13)	2.010(11)	2.011(6)	1.988(7)
Mo(1)−N(14)	2.215(10)	2.244(6)	2.236(6)
N(1)−N(2)	1.164(13)	1.217(7)	1.249(8)
N(3)−N(4)	1.193(13)	1.221(7)	1.245(8)
M−N(2)	1.973(11)	1.864(4)	1.978(6)
M−N(4)	1.966(11)	1.860(6)	1.974(6)
Mo(1)−N(1)−N(2)	175.6(9)	178.2(5)	176.9(5)
N(2)−M−N(4)	134.7(5)	119.8(3)	114.6(2)
M−N(2)−N(1)	178.2(9)	169.2(5)	175.9(6)
M−N(4)−N(3)	166.6(9)	172.1(5)	170.6(5)
other	2.041(10) (Mg−O(1))	2.061(5) (V−O)	2.394(2) (Zr−Cl(1))
	2.019(10) (Mg−O(2))	2.288(2) (V−Cl)	2.408(2) (Zr−Cl(2))
	94.7(5) (O(1)−Mg−O(2))	96.5(2) (O−V−Cl)	107.14(9) (Cl(1)−Zr−Cl(2))
	107.9(4) (N(2)−Mg−O(1))	114.9(2) (Cl−V−N(2))	108.5(2) (Cl(1)−Zr−N(2))
	104.5(4) (N(2)−Mg−O(2))	114.9(2) (Cl−V−N(2))	108.7(2) (Cl(1)−Zr−N(4))
	105.1(4) (N(4)−Mg−O(1))	104.2(2) (O−V−N(4))	109.4(2) (Cl(2)−Zr−N(2))
	102.8(4) (N(4)−Mg−O(2))	119.8(3) (N(2)−V−N(4))	108.3(2) (Cl(2)−Zr−N(4))

[a] See refs 1 and 2. [b] Selected distances and angles for only one $[N_3N]Mo(N_2)$ unit are listed. See Supporting Information for a full list of distances and angles.

avoid redox chemistry by employing halides of earlier transition metals such as zirconium.

$\{[N_3N]Mo(N_2)\}_2Mg(THF)_2$ reacts cleanly with 2 equiv of $ZrCl_4(THF)_2$ in THF to give $\{[N_3N]Mo{-}N{=}N\}ZrCl_3(THF)_2$ (**5**) as salmon-colored needles in 77% yield (eq 9). The ^{1}H NMR spectrum of diamagnetic **5** in THF-d_8, consists of a single TMS resonance and a pair of pseudo triplets for the methylene protons on the ligand backbone characteristic of compounds in which the $[N_3N]Mo$ portion of the molecule is C_3-symmetric. Resonances attributed to coordinated THF are also observed in the spectrum, and elemental analyses are consistent with there being two molecules of THF present per zirconium center. The IR spectrum of **5** in Nujol has a broad N−N absorption at 1515 cm^{-1}, which is within the range reported for related group 4 heterobimetallic bridging dinitrogen complexes (1468−1545 cm^{-1}).[23]

$$\{[N_3N]Mo{-}N{=}N\}_2Mg(THF)_2 + 2ZrCl_4(THF)_2 \xrightarrow[-\ MgCl_2]{THF} 2\{[N_3N]Mo{-}N{=}N\}ZrCl_3(THF)_2 \quad (9)$$
5

Reaction of $\{[N_3N]Mo(N_2)\}_2Mg(THF)_2$ with $ZrCl_4(THF)_2$ in a 1:1 ratio yields the diamagnetic complex $\{[N_3N]Mo(N_2)\}_2ZrCl_2$ (**6**) as red cubes in moderate yield (54%, eq 10). The ^{1}H NMR

$$\{[N_3N]Mo{-}N{=}N\}_2Mg(THF)_2 + ZrCl_4(THF)_2 \xrightarrow[-\ MgCl_2]{THF} \{[N_3N]Mo{-}N{=}N\}_2ZrCl_2 \quad (10)$$
6

spectrum of **6** in C_6D_6 reveals the presence of 1 equiv of THF per zirconium center, an observation that is corroborated by elemental analysis data. Since an X-ray structure of **6** (crystallized from ether; see below) shows it to be a pseudotetrahedral species, it is not known whether THF is coordinated to Zr in the original sample or not. The IR spectrum of **6** in Nujol is characterized by a strong N−N absorption at 1556 cm^{-1}.

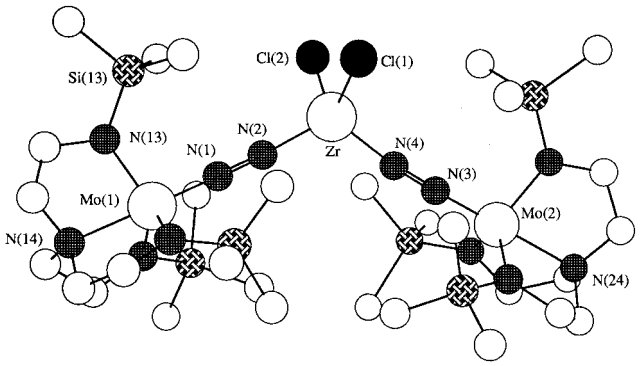

Figure 5. View of the structure of $\{[N_3N]Mo{-}N{=}N\}_2ZrCl_2$ (**6**).

Compound **6** (with one THF present) slowly disproportionates in solution to give **5** and $\{[N_3N]Mo(N_2)\}_3ZrCl$ (**7**, see below); after 48 h ^{1}H NMR spectra of C_6D_6 solutions indicate that **5**, **6**, and **7** are present in an approximate ratio of 1:3:1.

Single crystals of **6** were grown from saturated diethyl ether solutions at −20 °C and examined in an X-ray study; one-half molecule of diethyl ether was found in the unit cell. Crystallographic data are given in Table 1. The molecular structure of **6** along with the atom-labeling scheme is shown in Figure 5 while selected bond lengths and bond angles are listed in Table 3. The Mo−N−N and Zr−N−N linkages are essentially linear, as expected. The relatively large size of Zr(IV) (0.84 Å[18]) along with the relatively long Zr−N bond lengths leads to facile accommodation of two sterically bulky $[N_3N]Mo(N_2)$ ligands, as reflected in a N(2)−Zr−N(4) bond angle of only 114.6(2)°. The Mo−N_α bond lengths at 1.797(6) and 1.796(6) Å are the shortest of all the crystallographically characterized heterobimetallic complexes reported here. The N−N bond lengths in **6** are approximately what they are in the related heterobimetallic dinitrogen complex $WI(PMe_2Ph)_3(py)(\mu\text{-}N_2)ZrCp_2Cl$ (1.24(2) Å)[23] but only slightly longer than what they are in **4**.

The reaction between $ZrCl_4(THF)_2$ and 1.5 equiv of $\{[N_3N]Mo(N_2)\}_2Mg(THF)_2$ led to the formation of $\{[N_3N]Mo(N_2)\}_3ZrCl$ (**7**), which could be isolated as deep red needles from diethyl ether in 68% yield. Proton and carbon NMR spectra of **7** are similar to spectra of **5** and **6** and again characteristic of

(23) Mizobe, Y.; Yokobayashi, Y.; Oshita, H.; Takahashi, T.; Hidai, M. *Organometallics* **1994**, *13*, 3764.

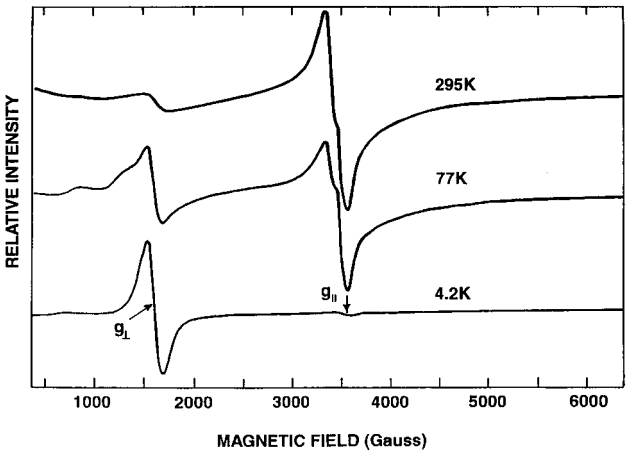

Figure 6. Temperature dependence of the X-band ESR spectrum of $\{[N_3N]Mo(N_2)\}_3Fe$ (**1**).

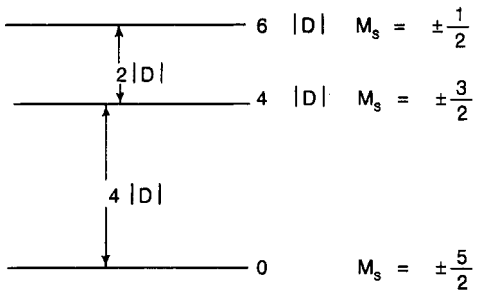

Figure 7. Negative axial zero field splitting for spin sextet Fe(III).

a complex in which the $[N_3N]Mo$ portion of the molecule is C_3-symmetric. The IR spectrum of **7** taken in Nujol has a strong broad absorption at 1576 cm^{-1}. Solutions of **7** in C_6D_6 show no signs of decomposition or disproportionation when stored at room temperature under dinitrogen for 72 h (according to ^1H NMR spectroscopy).

Efforts to prepare $\{[N_3N]Mo(N_2)\}_4Zr$ were unsuccessful, however. Reaction of $ZrCl_4(THF)_2$ with 2 equiv of $\{[N_3N]Mo(N_2)\}_2Mg(THF)_2$ yielded **7** as the sole identifiable product. These results suggest that $\{[N_3N]Mo{-}N{=}N\}_4Zr$ is not accessible on steric grounds. This fact is consistent with the stability of compound **7** toward disproportionation to **6** and $\{[N_3N]Mo(N_2)\}_4Zr$.

Mössbauer, EPR, and Magnetic Susceptibility Studies of Iron/Molybdenum Complexes. The ambiguity concerning whether $\{[N_3N]Mo(N_2)\}$ or $\{[N_3N]Mo(N_2)\}^-$ is a better description of the ligand in a situation where the metal to which the ligand is bound can be in a more reduced state (with a neutral ligand) or a more oxidized state (with an anionic ligand) led to a detailed exploration of the X-band ESR, iron-57 Mössbauer spectroscopy, and magnetic susceptibility of the iron−molybdenum complexes reported here.

Studies of **1** unequivocally confirm that it contains high-spin Fe(III) in an anisotropic magnetic environment. The total absence of axial ligation leads to an unusually large electric field gradient at the high-spin Fe(III) centers (quadrupole splitting = 2.93 mm/s at ambient *T* and 3.15 mm/s at 77 K) and the expected classical (near axial) X-band ESR spectral pattern, i.e., $g_{EFF}(\perp) \sim 6$, $g_{EFF}(\parallel) \sim 2$ (Figure 6). The corresponding zero field splitting, *D*, of **1** is negative (Figure 7), as suggested by the progressive broadening of its zero field Mössbauer spectrum with *decreasing temperature* (Figure 8), owing to slow paramagnetic relaxation in its ground state doublet. Relaxation in the $\pm^1/_2$ doublet is fully allowed and

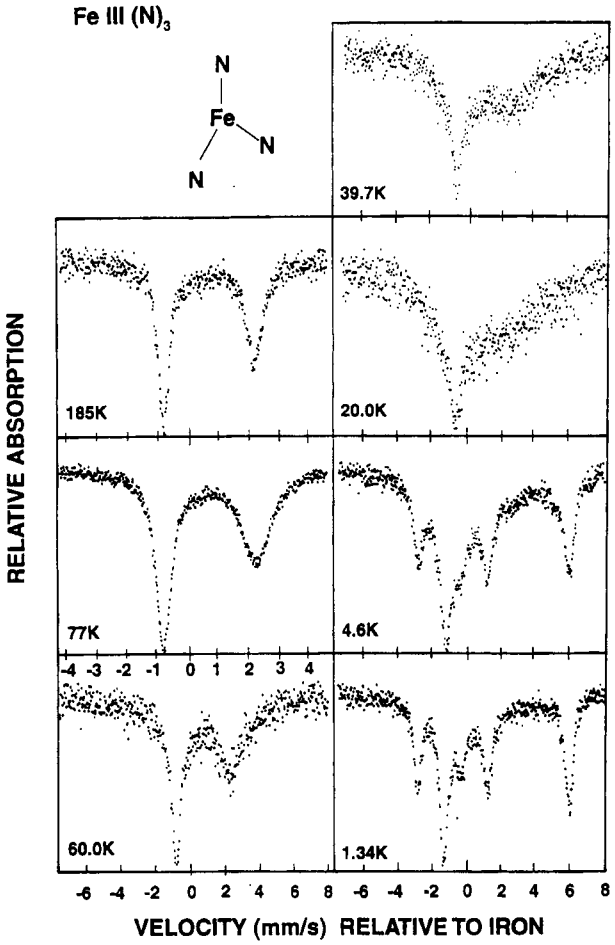

Figure 8. Temperature dependence of the zero field Mössbauer spectra of $\{[N_3N]Mo(N_2)\}_3Fe$ (**1**).

rapid. There is little doubt that the principal component of the electric field gradient tensor ($\mathbf{V}_{zz}$) is *positive* for **1** on the basis of simple point charge model calculations[24] and the fact that there is relatively strong in-plane bonding and no axial ligation. Thus the observed details[25] of its slow paramagnetic relaxation broadening indicate internal hyperfine field fluctuations *parallel* to the local 3-fold symmetry axis and that of $\mathbf{V}_{zz}$.

Specifically, when $\mathbf{V}_{zz}$ is *positive*, the $|^1/_2, \pm^1/_2\rangle \rightarrow |^3/_2, \pm^3/_2\rangle$ γ-ray transition is highest in energy (occurs at higher velocity).[24] Longitudinal relaxation, i.e., parallel to the local highest fold symmetry axis (and that of $\mathbf{V}_{zz}$) causes *initial* broadening of the foregoing transition, while transverse relaxation causes the $|^1/_2, \pm^1/_2\rangle \rightarrow |^3/_2, \pm^1/_2\rangle$ (lower velocity transition) to broaden first. From Figure 8, it is clear that the former transition suffers initial broadening as *T* decreases. The Zeeman spectrum (in zero applied field) at 1.34 K corresponds to essentially infinitely slow paramagnetic relaxation. The limiting saturation value for the internal hyperfine field H_N is estimated as ~28 T. This value is somewhat larger than that (17.5 T) observed[26] at 1.5 K for $Fe[N(SiMe_3)_2]_3$. To our knowledge, the latter complex is the sole other trigonal planar high-spin Fe(III) system[6,7,26] to be characterized in detail via Mössbauer spectroscopy. Amazingly, its quadrupole splitting (+5.12 mm/s) is even larger than observed in **1**. Perhaps this suggests a substantially stronger interaction of the amido

(24) Greenwood, N. N.; Gibb, T. C. *Mössbauer Spectroscopy*; Chapman and Hall: London, 1972.
(25) Blume, M. *Phys. Rev. Lett.* **1965**, *14*, 96.
(26) Fitzsimmons, B. W.; Johnson, C. E. *Chem. Phys. Lett.* **1974**, *24*, 422.

nitrogen atoms with the ferric center in $Fe[N(SiMe_3)_2]_3$ than in **1**, although the available crystallographic data seem to suggest the reverse, i.e., Fe−N = 1.92 Å[6] for $Fe[N(SiMe_3)_2]_3$ and 1.85 Å for **1**.

At the other extreme is the trigonal bipyramidal penta-azido complex, $[Ph_4As]_2[Fe(N_3)_5]$.[27] This system has an isomer shift (relative to iron) of 0.56 mm/s (78 K), similar to what is found here. However its quadrupole splitting is much smaller (0.75 mm/s). This value is much more typical of the near spherical ^{6}A core of (e.g.) octa- or tetrahedrally coordinated high-spin Fe(III), which can with 6 or 4 equiv ligands exhibit near-zero quadrupole splitting. Put simply, the two additional axial ligands of the five-coordinate system largely counter-balance the electric field gradient produced by the trigonally arrayed in-plane ligands leading to an overall smaller quadrupole splitting effect.

One can now qualitatively consider the fundamental contributions to H_N and rationalize the unusually small values of H_N observed for the present three-coordinate system and $Fe[N(SiMe_3)_2]_3$ versus $[Ph_4As]_2[Fe(N_3)_5]$. The internal hyperfine field in zero external field is given by the equation $H_N = H_F + H_L + H_D$.[24] H_F, the Fermi contact contribution, is usually dominant for high-spin Fe(III) (∼11 T per spin). This leads to the expectation $H_N \approx 55$ T for high-spin Fe(III) with its 5 spins. However, owing to convalency−delocalization reduction effects, observed values for H_N typically range between 44 and 50 T.

H_L is the orbital contribution which is expected to be negligible for ^{6}A ground-state ferric while H_D is the so-called dipolar contribution. This term happens to scale as the magnitude of the principal component of the electric field gradient tensor, i.e., basically the quadrupole interaction. Both H_D and H_L are usually of opposite sign to H_F. Thus the three-coordinate systems appear to have substantial opposing dipolar contributions relative to H_F resulting in highly reduced values of H_N. On the other hand, the penta-azido system with its significantly smaller quadrupole splitting exhibits an $H_N = 48.7$ T,[28] which is much closer to the full Fermi contact contribution, but with some covalency reduction effects. This is clearly more typical behavior for spin sextet iron III.

Compound **1** is a relatively self-dilute magnetic system. The smallest Fe(III)−Fe(III) separation in **1** is 10.5 Å. This ultimately leads to the long spin−spin relaxation[29] times requisite to the observation of slow paramagnetic relaxation and resolved magnetic hyperfine splitting. Finally, the chemical isomer shift (δ) of **1** (relative to natural iron foil) is 0.65 mm/s, fully consistent with spin sextet Fe(III).

The temperature dependence of the ESR spectra (Figure 6) corresponds to a complex competition between spin−lattice relaxation broadening effects at higher temperature and progressive depopulation of the ESR transition allowed $M_s = \pm 1/2$ Kramers doublet with decreasing temperature. Recall that the $M_s = \pm 3/2$ and $M_s = \pm 5/2$ doublets are ESR silent as they correspond to highly forbidden $\Delta M_s = \pm 3$ and ± 5 transitions, respectively. These complications not withstanding, it will be seen that the overall behavior strongly suggests that D is in fact negative, consistent with the temperature dependence of the Mössbauer spectra. Qualitatively while the $g \sim 2$ signal appears intense, the lower field transition is apparently more highly broadened as a result of spin−lattice effects. On decreasing the temperature to ∼77 K and concomitantly reducing phonon (lattice-vibrational) excitation, such broadening

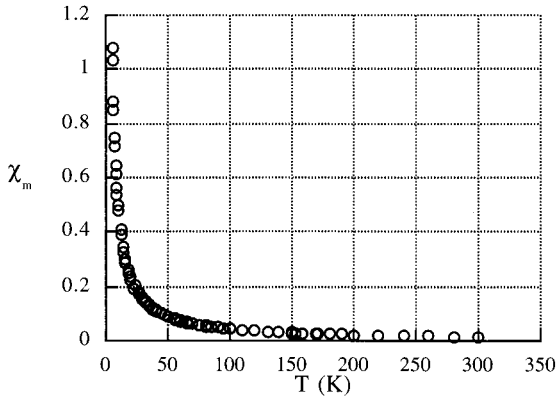

Figure 9. Plot of χ_m (corrected for diamagnetism using Pascal's constants) versus T for $\{[N_3N]Mo-N{=}N\}_3Fe$ (**1**).

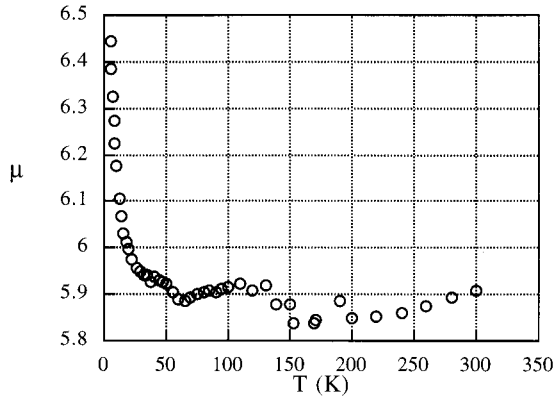

Figure 10. Plot of μ versus T for $\{[N_3N]Mo-N{=}N\}_3Fe$ (**1**).

effects should lessen. It is seen that the lower field transition has "sharpened-up" and additional features likely corresponding to rhombicity of the g tensor are now evident. In the limit of very low temperature (4.2 K), the $M_s = \pm 1/2$ is further depopulated leading to a decrease in the relative intensity (I) of the $g(\|)$ signal. However, statistically for random polycrystalline powder samples, $I(g(\perp))$ is generally expected to be greater than $I(g(\|))$.

SQUID magnetic susceptibility data for solid **1** is plotted versus temperature in Figure 9 and can be fit to the Curie−Weiss law ($\chi = \mu^2/8(T - \theta)$) over the temperature range 5−300 K to yield $\mu = 6.02(3)\ \mu_B$, $\theta = 0.74(5)$ K. The value of μ is consistent with the expected spin-only value for a system containing five unpaired electrons (5.92 μ_B) and with formulation of **1** as a high-spin Fe(III) complex. On the other hand, a careful look at the corresponding variation in the effective magnetic moment of **1** (Figure 10) suggests features relevant to the proceeding discussion of the Mössbauer and ESR spectra. Above ∼50 K, μ exhibits some scatter but is generally close to $\sqrt{35}$ i.e., the spin-only value expected for high-spin ($S = 5/2$) Fe(III). Below ∼50 K, the moment commences to diverge strongly, rising to near 6.5 μ_B at 4.2 K. Precisely this type of moment behavior is theoretically predicted[30] for axially distorted anisotropic, high-spin Fe(III) centers when studied as single crystals. However, even for polycrystalline powder samples, if the magnetic anisotropy is large for a high-spin system, the moderate applied fields (0.1−0.5 T) used in typical DC susceptibility studies are sufficient to fully magnetically align the sample along the largest principal moment direction ($\mu_\|$or $\mu_\perp$) to give oriented single crystal behavior. This effect is

(27) Drummond, J.; Wood, J. S. *Chem. Commun.* **1969**, 1373.
(28) Reiff, W. M.; Wong, H.; Tuiroc, M.; Eisman, G. *J. Phys. Colloq.* **1979**, *40* (C2), 234−236.
(29) Wignal, J. W. G. *J. Chem. Phys.* **1968**, *44*, 2462.
(30) Gerloch, M.; Lewis, J.; Slade, R. C. *J. Chem. Soc. (*A) **1969**, 1422.

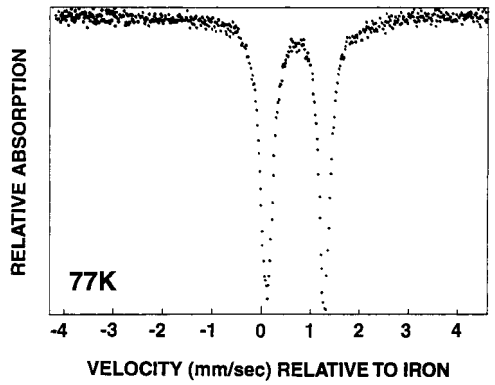

Figure 11. Mössbauer spectrum of $\{[N_3N]Mo(N_2)\}_2Fe(DMPE)$ (**2**).

particularly pronounced for high-spin Fe(III) for the case $\mu_{||} > \mu_{\perp}$ and $D < 0$ leading to μ values maximizing at $\sim 8\ \mu_B$ before ultimately decreasing at very low temperatures. In this context the effective moment of "powder samples"[28] of the previously mentioned $[Ph_4As]_2[Fe(N_3)_5]$ for which $D \sim -1\ cm^{-1}$ reaches 7.4 μ_B at 5 K and then decreases to $\sim 6\ \mu_B$ at 1.6 K in a field of ~ 0.5 T. Such magnetic polarization effects are undoubtedly occurring for the present tricoordinate ferric system ($H_o = 1$ T) and are further evidence for a large negative axial zero field parameter, D, of ~ -0.5 to $\sim 1\ cm^{-1}$ (~ 1 to 1.5 K).

The Mössbauer spectra of $\{[N_3N]Mo{-}N{=}N\}_2Fe(DMPE)$ (**2**) are far less complex than those of **1**. The Mössbauer spectrum of **2** exhibits a near symmetric quadrupole doublet ($\Delta E = 1.18$ mm/s) (Figure 11) and isomer shift (0.67 mm/s at 77 K) consistent with Fe(II) in a highly covalent pseudotetrahedral environment.[24] SQUID magnetic susceptibility studies have been carried out on solid **2** and the data can be fit to the Curie−Weiss law ($\chi = \mu^2/8(T - \theta)$) over the temperature range 50−300 K to yield $\mu = 5.08(3)\ \mu_B$, $\theta = 2.4(6)$ K, data that are also consistent with **2** being a high-spin Fe(II) complex.

Conclusions

We have demonstrated that $\{[N_3N]Mo(N_2)\}^-$ can be employed as a ligand in the synthesis of heterobimetallic dinitrogen complexes from transition metal halides and $\{[N_3N]Mo(N_2)\}_2Mg(THF)_2$. Since the $\{[N_3N]Mo(N_2)\}^-$ ligand can exist also in a neutral form, and $\{[N_3N]Mo(N_2)\}^-$ is a reasonably good reducing agent, interconversion of Fe^{II}/Fe^{III} and V^{III}/V^{IV} dinitrogen complexes is relatively facile, and efforts to prepare a given complex in high yield therefore complicated to a significant degree. Mössbauer studies of $\{[N_3N]Mo{-}N{=}N\}_3Fe$ and $\{[N_3N]Mo{-}N{=}N\}_2Fe(DMPE)$ clearly establish oxidation states of Fe(III) and Fe(II), respectively. On this basis we can conclude that the complexes examined so far contain the $\{[N_3N]Mo(N_2)\}^-$ ligand, a relative of the N_3^- ligand, not $[N_3N]Mo(N_2)$. It is clear that $\{[N_3N]Mo(N_2)\}^-$ complexes can be prepared readily when the metal is not prone to reduction (e.g., for Zr(IV)) and that only three $\{[N_3N]Mo(N_2)\}^-$ ligands can be accommodated at a given metal center for steric reasons.

Experimental Procedures

General Details. All experiments were performed under a nitrogen atmosphere in a Vacuum Atmospheres drybox or by standard Schlenk techniques unless otherwise specified. Pentane was washed with sulfuric acid/nitric acid (95/5 v/v), sodium bicarbonate, and water, stored over calcium chloride, and distilled from sodium benzophenone ketyl under nitrogen. Toluene was distilled from sodium, and CH_2Cl_2 was distilled from CaH_2. Anhydrous diethyl ether and THF were sparged with nitrogen and passed through alumina columns.[31] All solvents were stored in the drybox over activated 4 Å molecular sieves.

NMR data were obtained at 300 or 500 MHz (^1H), 75.4 MHz (^{13}C), and 121.8 MHz (^{31}P) and are listed in parts per million downfield from tetramethylsilane for proton and carbon and in parts per million downfield from 85% H_3PO_4 for phosphorus. Coupling constants are listed in Hertz. Spectra were obtained at 25 °C unless otherwise noted. Benzene-d_6 and toluene-d_8 were predried on CaH_2, vacuum transferred onto sodium and benzophenone, stirred under vacuum for 2 days, then vacuum-transferred into small storage flasks, and stored over molecular sieves. $[N_3N]MoCl$,[3] $Fe(DMPE)Cl_2$,[32] $VCl_3(THF)_3$,[33] $VCl_4(DME)$,[34] and $ZrCl_4(THF)_2$[33] were prepared as described in the literature. $FeCl_2$ and $FeCl_3$ were purchased from commercial vendors and used as received.

UV/visible spectra were recorded on a HP 8452 diode array spectrophotometer using a Hellma 221-QS quartz cell (path length = 10 mm) sealed to a gas adapter fitted with a Teflon stopcock. IR spectra were recorded on a Perkin-Elmer 1600 FT-IR spectrometer. Elemental analyses (C, H, N) were performed in our laboratory using a Perkin-Elmer 2400 CHN analyzer or by Microlytics Analytical Laboratories of Deerfield MA. X-ray data were collected on Siemens SMART/CCD diffractometer and the structures were solved without complications as described in the literature.[35] Details can be found in the Supporting Information.

SQUID Magnetic Susceptibility Measurements. Measurements were carried out on a Quantum Design SQUID magnetometer. Data were obtained at a field strength of 5000 G. Straws and gel caps (Gelatin Capsule No. 4 Clear) were purchased from Quantum Design. The sample was prepared in the drybox by the following method. A gel cap and a square of Parafilm were weighed. The sample was placed in the gel cap, and the Parafilm inserted above it. The gel cap was closed, and the mass of the sample was ascertained by weighing the loaded gel cap. The gel cap was placed in a straw which was then mounted on the sample rod and placed in the magnetometer. Two runs were performed on the sample: one from 5 to 300 K and a second from 300 to 5 K. Measurements were made at the following increments: 5−10 K (every 1 K), 10−20 K (every 2 K), 20−50 K (every 3 K), 50−100 K (every 5 K), 100−200 K (every 10 K), 200−300 K (every 20 K).

Mössbauer and X-Band ESR Studies. Variable temperature Mössbauer spectra were recorded using equipment that has been described previously in conjunction with a 100 mCi $^{57}Co(Rh)$ γ-ray source.[36] α-Iron foil was employed as a standard. The spectra were fit to Lorentzians, using a program written primarily by Stone.[37] Electron spin resonance spectra were measured with a Bruker model ESP-300E spectrometer. Low-temperature measurements employed an ESR-900 cryostat with iron−gold thermocouple.

$\{[N_3N]MoN_2\}_3Fe$ (1). $\{[N_3N]Mo(N_2)\}_2Mg(THF)_2$ (316 mg, 0.28 mmol) was dissolved in a mixture of 10 mL of diethyl ether, 2 mL of THF, and 1 mL of toluene and the solution was cooled to −20 °C. An $FeCl_2$ (35 mg, 0.28 mmol) slurry in 1 mL of ether, was cooled to −20 °C and then added all at once to the stirred solution of $\{[N_3N]Mo(N_2)\}_2Mg(THF)_2$. Over the course of 15 min $FeCl_2$ was taken into solution as the color of the solution darkened to a burnt orange color. After 90 min the solvent was removed to give a black-purple residue. This residue was extracted with 30 mL of pentane and the purple solution was filtered through Celite. When the volume of the pentane solution was decreased in vacuo purple crystals began to form. The solution was cooled to −20 °C and the black-purple crystalline product was filtered off; yield 105 mg (38%). ^1H NMR (C_6D_6): δ 9.25 ($\Delta\nu_{1/2}$ =

(31) Pangborn, A. B.; Giardello, M. A.; Grubbs, R. H.; Rosen, R. K.; Timmers, F. J. *Organometallics* **1996**, *15*, 1518.
(32) Girolami, G. S.; Wilkinson, G.; Galas, A. M. R.; Thorton-Pett, M.; Hursthouse, M. B. *J. Chem. Soc., Dalton Trans.* **1985**, 1339.
(33) Manzer, L. E. *Inorg. Synth.* **1982**, *21*, 135.
(34) Bridgland, B. E.; Fowles, G. W. A.; Walton, R. A. *J. Inorg. Nucl. Chem.* **1965**, *27*, 383.
(35) Rosenberger, C.; Schrock, R. R.; Davis, W. M. *Inorg. Chem.* **1997**, *36*, 123.
(36) Chang, C.; Reiff, W. *Inorg. Chem.* **1977**, *16*, 297.
(37) Bancroft, G.; Maddock, A.; Ong, W.; Prince, R.; Stone, A. *J. Chem. Soc. A* **1967**, 1966.

705 Hz, $SiMe_3$), −9.71 ($\Delta\nu_{1/2}$ = 288 Hz, NCH_2CH_2N), −64.0 ($\Delta\nu_{1/2}$ = 241 Hz, NCH_2CH_2N). IR (Nujol, cm^{-1}): 1703 (N═N); UV−visible (pentane) λ = 516 nm, ϵ = 22 818 M^{-1} cm^{-1}. SQUID: μ = 6.03 μ_B. Elemental analyses were thwarted by the presence of traces of $[N_3N]Mo(N_2)$ that could not be separated from **1**.

{[N$_3$N]MoN$_2$}$_2$Fe(DMPE)·Ether (2). $\{[N_3N]Mo(N_2)\}_2Mg(THF)_2$ (454 mg, 0.40 mmol) was dissolved in 10 mL of THF, and the solution was cooled to −20 °C. $FeCl_2$ (51 mg, 0.40 mmol) was added all at once to the stirred solution. After 1 min the solution began to darken in color and took on a dark burnt-orange color. After 45 min the solvent was removed in vacuo and the residue extracted with 40 mL of pentane. The purple pentane solution was filtered through Celite and the pentane removed to give a black-purple solid. This solid was dissolved in 10 mL of toluene and DMPE (60 mg, 0.40 mmol) in 3 mL of toluene was added dropwise to the stirred solution. The reaction mixture was stirred for 20 min and the solvent was removed in vacuo. The residue was extracted with 15 mL of diethyl ether, the extract was filtered, and the volume of the filtrate was reduced to 7 mL. Upon cooling this solution to −20 °C the product was obtained as black blocks; yield 200 mg (43%). ^{1}H NMR (C_6D_6): δ 37.0 (P(CH_3)$_2$ or PCH_2), 6.62 ($\Delta\nu_{1/2}$ = 690 Hz, $SiMe_3$), −4.67 ($\Delta\nu_{1/2}$ = 337 Hz, NCH_2CH_2N), −47.43 ($\Delta\nu_{1/2}$ = 591 Hz, NCH_2CH_2N), −117.46 (P(CH_3)$_2$ or PCH_2). IR (Nujol, cm^{-1}): 1706 (N═N). UV−visible (pentane): λ = 360 nm, ϵ = 23 306 M^{-1} cm^{-1}; λ = 508 nm, ϵ = 13 997 M^{-1} cm^{-1}. SQUID: μ = 5.08 μ_B. Anal. Calcd for $C_{40}H_{104}N_{12}Si_6Mo_2FeP_2O$: C, 38.51; H, 8.40; N, 13.47. Found: C, 38.55; H, 8.43; N, 13.53.

{[N$_3$N]MoN$_2$}$_3$VCl (3). Method 1. $\{[N_3N]Mo(N_2)\}_2Mg(THF)_2$ (300 mg, 0.264 mmol) was dissolved in 10 mL of THF and the solution was cooled to −20 °C. VCl_4(DME) (50 mg, 0.177 mmol) was dissolved in 3 mL of THF, and the solution was cooled to −20 °C and then added to the stirred solution of $\{[N_3N]Mo(N_2)\}_2Mg(THF)_2$. The mixture was stirred for 15 h to give a purple solution. The solvent was removed and the residue was extracted with 15 mL of toluene. The mixture was filtered through Celite and the toluene was removed in vacuo. The resulting residue was recrystallized from THF/pentane to give the product as black plates; yield 112 mg (42%).

Method 2. A solution of $\{[N_3N]Mo(N_2)\}_2Mg(THF)_2$ (290 mg, 0.255 mmol) in 7 mL THF was cooled to −20 °C and a cooled solution of $VCl_3(THF)_3$ (95 mg, 0.255 mmol) in 2 mL THF was then added with stirring. The reaction mixture was stirred for 25 h to give a purple solution. The solvent was removed in vacuo and the residue was extracted with 15 mL of toluene. The extract was filtered through Celite and the toluene was removed in vacuo. The resulting residue was recrystallized from THF/pentane to give the product as black plates; yield 108 mg (28%). ^{1}H NMR (C_6D_6): δ 1.36 ($\Delta\nu_{1/2}$ = 20 Hz, NCH_2CH_2N), 0.94 ($\Delta\nu_{1/2}$ = 6 Hz, $SiMe_3$), −0.55 ($\Delta\nu_{1/2}$ = 14 Hz, NCH_2CH_2N). IR (Nujol, cm^{-1}): 1579 (N═N). SQUID: μ = 1.50 μ_B.

{[N$_3$N]Mo(N$_2$)}ZrCl$_3$(THF)$_2$ (5). $ZrCl_4(THF)_2$ (100 mg, 0.265 mmol) was added as a solid to the stirred solution of $\{[N_3N]Mo(N_2)\}_2Mg(THF)_2$ (150 mg, 0.136 mmol) in 7 mL of THF that had been cooled to −20 °C. After 3 h, the solvent was removed in vacuo and the residue was extracted with 15 mL of toluene. The mixture was filtered through a pad of Celite and the toluene was removed from the filtrate under reduced pressure. The residue was recrystallized from THF/pentane to afford the product as salmon-colored needles; yield 153 mg (77%). ^{1}H NMR (THF-d_8): δ 3.75 (t, NCH_2CH_2N), 3.62 (m, THF), 2.90 (t, NCH_2CH_2N), 1.78 (m, THF), 0.35 (s, $SiMe_3$); ^{13}C{^{1}H} NMR (THF-d_8) δ 68.4 (THF), 54.9 (NCH_2CH_2N), 53.4 (NCH_2CH_2N), 26.5 (THF), 4.2 ($SiMe_3$). IR (Nujol, cm^{-1}): 1515 (N═N). Anal. Calcd for $C_{23}H_{55}N_6Si_3MoZrCl_3O_2$: C, 33.46; H, 6.72; N, 10.18, Cl, 12.88. Found: C, 33.90; H, 6.54; N, 9.81, Cl, 12.81.

{[N$_3$N]Mo(N$_2$)}$_2$ZrCl$_2$·THF (6). Compound **6** was prepared as described for **5** from $\{[N_3N]Mo(N_2)\}_2Mg(THF)_2$ (300 mg, 0.264 mmol) and $ZrCl_4(THF)_2$ (100 mg, 0.265 mmol) with a 29 h reaction time. The product was crystallized from a mixture of THF and pentane as red cubes; yield 160 mg (54%, 2 crops). ^{1}H NMR (C_6D_6): δ 3.60 (m, THF), 3.29 (t, NCH_2CH_2N), 2.04 (t, NCH_2CH_2N), 1.40 (m, THF), 0.65 (s, $SiMe_3$). ^{13}C{^{1}H} NMR (C_6D_6): δ 54.2 (NCH_2CH_2N), 52.5 (NCH_2CH_2N), 26.1 (THF), 4.5 ($NSiMe_3$); IR (Nujol, cm^{-1}) 1556 (N═N). Anal. Calcd for $C_{34}H_{86}N_{12}Si_6Mo_2ZrCl_2O$: C, 33.98; H, 7.21; N, 13.99. Found: C, 33.51; H, 7.21; N, 14.00.

{[N$_3$N]Mo(N$_2$)}$_3$ZrCl (7). Compound **7** was prepared as described for **5** from $\{[N_3N]Mo(N_2)\}_2Mg(THF)_2$ (155 mg, 0.136 mmol) dissolved in 5 mL of a 2:1 ether/toluene solution at −20 °C with a reaction time of 17 h. The product was crystallized from diethyl ether as deep red needles; yield 97 mg (68%). ^{1}H NMR (C_6D_6): δ 3.37 (t, NCH_2CH_2N), 2.10 (t, NCH_2CH_2N), 0.69 (s, $SiMe_3$). ^{13}C{^{1}H} NMR (C_6D_6): δ 55.0 (NCH_2CH_2N), 52.0 (NCH_2CH_2N), 4.7 ($NSiMe_3$). IR (Nujol, cm^{-1}): 1576 (N═N).

Acknowledgment. R.R.S. is grateful to the National Institutes of Health (GM 31978) for research support and also thanks the National Science Foundation for funds to help purchase a departmental Siemens SMART/CCD diffractometer. W.M.R. thanks Dr. Ralph Weber of Bruker Instruments, Billerica, MA, for obtaining the temperature dependent X-band ESR spectra.

Supporting Information Available: X-ray crystallographic files, in CIF format, for complexes **4** and **6** are available free of charge via the Internet at http://pubs.acs.org. Supporting Information for **1** can be found in the preliminary communication.[2]

IC9811188